PNAS RESEARCH ARTICLE | DEVELOPMENTAL BIOLOGY APPLIED MATHEMATICS OPEN ACCESS

A dynamical model of growth and maturation in *Drosophila*

John J. Tyson[a,1], Amirali Monshizadeh[b], Stanislav Y. Shvartsman[c,d], and Alexander W. Shingleton[b,1]

Edited by Lynn Riddiford, University of Washington, Friday Harbor, WA; received August 28, 2023; accepted October 12, 2023

The decision to stop growing and mature into an adult is a critical point in development that determines adult body size, impacting multiple aspects of an adult's biology. In many animals, growth cessation is a consequence of hormone release that appears to be tied to the attainment of a particular body size or condition. Nevertheless, the size-sensing mechanism animals use to initiate hormone synthesis is poorly understood. Here, we develop a simple mathematical model of growth cessation in *Drosophila melanogaster*, which is ostensibly triggered by the attainment of a critical weight (CW) early in the last instar. Attainment of CW is correlated with the synthesis of the steroid hormone ecdysone, which causes a larva to stop growing, pupate, and metamorphose into the adult form. Our model suggests that, contrary to expectation, the size-sensing mechanism that initiates metamorphosis occurs before the larva reaches CW; that is, the critical-weight phenomenon is a downstream consequence of an earlier size-dependent developmental decision, not a decision point itself. Further, this size-sensing mechanism does not require a direct assessment of body size but emerges from the interactions between body size, ecdysone, and nutritional signaling. Because many aspects of our model are evolutionarily conserved among all animals, the model may provide a general framework for understanding how animals commit to maturing from their juvenile to adult form.

growth cessation | body size | mathematical modeling | hormonal regulation | puberty

Significance

The decision to stop growth is critical in an animal's development. In humans and other species, this occurs at the onset of puberty, triggered by steroid hormone production that causes the transition from the juvenile to adult form. The factors triggering puberty are almost completely unknown but appear to be linked to reaching a specific body size, suggesting a size-sensing mechanism. This study focuses on fruit-fly metamorphosis, equivalent to puberty, which is ostensibly triggered by attaining a critical weight during larval development. Surprisingly, the study's mathematical model suggests that the critical-weight phenomenon does not directly reflect a size-sensing mechanism, but arises from interactions between body size, steroid hormones, and nutritional signaling that initiate metamorphosis earlier in development.

Body size is perhaps the most fundamental of all phenotypic traits, impacting an animal's morphology, physiology, behavior, and ecology (1, 2). The decision to stop growing and mature into an adult is therefore a critical point in development. In almost all animals, this decision is typically made some time before growth actually stops. In mammals, for example, the decision to stop growing is made at the onset of puberty, leading to upregulation of steroidogenesis and an irreversible transition from immature to adult form (3). Timely production of hormones, particularly steroids, also regulates the juvenile-to-adult transition in many other animals, including birds, amphibians, and insects (4–7). Despite intensive research into the developmental regulation of maturation hormones in multiple animals, how an animal knows when to initiate hormone synthesis so that it stops growing and completes maturation at the correct size remains poorly understood (8–11). Nevertheless, there is increasing evidence that initiation of the juvenile-to-adult transition is associated with the attainment of a particular body size or body condition in a wide variety of animals (9, 12–15).

In holometabolous insects such as the fruit fly *Drosophila melanogaster* and the tobacco hornworm *Manduca sexta,* the decision to stop growing is thought to reflect the attainment of a critical weight (CW) early in the final larval instar (16). Starving larvae smaller than the CW cause a delay in metamorphosis, while starving larvae greater than the CW do not. Based on this observation, attainment of CW is thought to trigger a size-sensing mechanism that ultimately and irreversibly up-regulates the synthesis of the molting hormone ecdysone by the prothoracic gland (PG). Increases in ecdysone titer initiate cessation of growth—fixing final body size—and drive metamorphosis into the adult form. Due to the experimental tractability of holometabolous insects, the critical-weight phenomenon has been extensively studied as a powerful model for understanding the mechanisms by which developing animals regulate the timing of maturation and final body size (17–22). Nevertheless, although we have a good understanding of the molecular and physiological mechanisms that regulate ecdysone synthesis (18, 23), the precise nature of the critical-weight phenomenon itself remains elusive. Specifically, it is unclear what size-sensing mechanism holometabolous insects use to initiate ecdysteroidogenesis and the extent to which this mechanism is evolutionarily conserved across species.

Developmental transitions, such as the onset of puberty or attainment of CW, are driven by underlying gene and endocrine regulatory networks that are governed, by and large, by the principles of gene expression and laws of biochemical kinetics. Such networks can be modelled (in a first approximation) by nonlinear differential equations. Recent theoretical proposals (24–29) have associated developmental transitions with bifurcations of nonlinear

Author affiliations: [a]Department of Biology, Virginia Polytechnic Institute and State University, Blacksburg, VA 24061; [b]Department of Biological Sciences, University of Illinois at Chicago, Chicago, IL 60607; [c]Department of Molecular Biology, Princeton University, Princeton, NJ 08544; and [d]Center for Computational Biology, Flatiron Institute, Simons Foundation, New York City, NY 10010

Author contributions: J.J.T., S.Y.S., and A.W.S. designed research; J.J.T., A.M., and A.W.S. performed research; J.J.T. and A.W.S. analyzed data; and J.J.T. and A.W.S. wrote the paper.

The authors declare no competing interest.

This article is a PNAS Direct Submission.

[1]To whom correspondence may be addressed. Email: tyson@vt.edu or ashingle@uic.edu.

This article contains supporting information online at https://www.pnas.org/lookup/suppl/doi:10.1073/pnas.2313224120/-/DCSupplemental.

Published November 28, 2023.

differential equations, which occur when a small change in a parameter induces a qualitative change in the long-term solution of the differential equations. In particular, irreversible decisions have been identified with saddle-node bifurcations of dynamical systems (30–32). The use of mathematical modeling to describe the hormonal regulation of growth cessation has, however, been underutilized. Such modeling promises to provide insight into the processes by which animals decide to stop growing in general, and the feasibility that this decision is causally linked to the attainment of a particular body size/condition specifically.

In this paper, we propose an alternative to the hypothesis that the critical-weight phenomenon involves a size-sensing mechanism that directly links body size to the commitment to adult maturation and cessation of body growth. Instead, using *Drosophila* as a model, we argue that the size-dependent developmental transition emerges due to the interactions between body size, ecdysone production, and nutritional signaling. We demonstrate how this is possible using a simple model of larval growth and ecdysone synthesis based on a pair of nonlinear ordinary differential equations. The model reproduces observed changes in body size and ecdysone levels during the third (final) instar of *Drosophila* larvae and precisely generates the phenomenological characteristics of a CW. Importantly, the decision to metamorphose is made much earlier in development than attainment of CW and corresponds most closely to the minimal viable weight (MVW) for pupariation. This suggests that the critical-weight phenomenon, as observed in *Drosophila* larvae at least, is not a direct consequence of a size-sensing mechanism but rather an indirect consequence of the physiological mechanisms that regulate growth and ecdysone synthesis.

Results

Biological Basis for the Model.

The critical-weight phenomenon. *D. melanogaster* are holometabolous insects that, after hatching, develop into mobile, feeding larvae, which grow dramatically, passing through three larval instars. In all holometabolous insects, a commitment is made in the final instar to stop feeding, pupate, and metamorphose into the adult form. Because growth of the adult body is prohibited by its hard exoskeleton, adult body size is largely determined by the size of the larva at pupation. The decision to pupate is, however, made much earlier in the final larval instar, ostensibly at attainment of a CW. This decision is associated with the production of the steroid hormone ecdysone (E), which initiates the cessation of feeding, the termination of larval growth, and, after some period, pupation and metamorphosis (Fig. 1*A*) (5, 16). Ecdysone also triggers final growth and differentiation of the imaginal discs, as well as autophagy of the fat body to support metamorphosis after the cessation of feeding (33–35). In well-fed larvae, *time-to-pupation* (TTP), the remaining larval period for a larva of a particular size or age, is a simple decreasing function of larval mass (Fig. 1*B*, green line) (36, 37). In contrast, starvation or suppressed nutritional signaling in small larvae (below CW) retards development and increases TTP (relative to well-fed larvae), while starvation or suppressed nutritional signaling in larger larvae (above CW) either does not affect TTP (for example in *M. sexta*) (37) or accelerates development and decreases TTP (in *Drosophila*) (36). CW is therefore operationally defined as a change in the relationship between mass at starvation and TTP (Fig. 1*B*, red line) (36, 37), and is thought to reflect a size-sensing switch at which a larva commits to metamorphose without the necessity of further growth (5, 37, 38). The precise mechanism of the switch remains unknown, although, as described below, several factors that regulate ecdysteroidogenesis also influence CW in *Drosophila.*

The regulation of ecdysone synthesis. The signaling pathways that regulate ecdysone synthesis are described in great detail in recent review articles by Texada et al. (18) and Kannangara et al. (23). While there are many regulators of ecysteroidogenesis in the PG, we focus on three key signaling pathways that appear to affect the critical-weight phenomenon: insulin/insulin-like growth factor signaling (IIS), prothoracicotropic hormone (PTTH) signaling, and ecdysone signaling (Fig. 2*A*). The IIS pathway is activated by circulating insulin-like peptides (ILPs) released, in part, in a nutrient-dependent manner from insulin-producing cells in the brain (40). The ILPs bind to the insulin receptor of cells and activate the IIS pathway, which promotes systemic growth by repressing the Forkhead Box subfamily O transcription factor (FOXO), a negative growth regulator (41, 42). In the PG, FOXO suppresses the expression of ecdysone-biosynthesis genes, so the repression of FOXO by IIS increases ecdysteroidogenesis (21), although IIS may also activate ecdysteroidogenesis through other mechanisms (43). PTTH, released from neurosecretory cells that project from the brain to the PG, is regulated by the developmental status of the imaginal tissue and circadian phase (44). PTTH activates the Ras/Raf/Mitogen-activated protein kinase (MAPK) pathway via its receptor Torso to up-regulate ecdysteroidogenesis (45). PG-autonomous activation of both IIS and PTTH signaling accelerates pupation and reduces adult body size, ostensibly by reducing CW, while suppression has the opposite effect (46, 47). Ecdysone is known to positively regulate its own synthesis via two mechanisms. First, ecdysone, or rather its metabolite 20-hydroxyecdysone

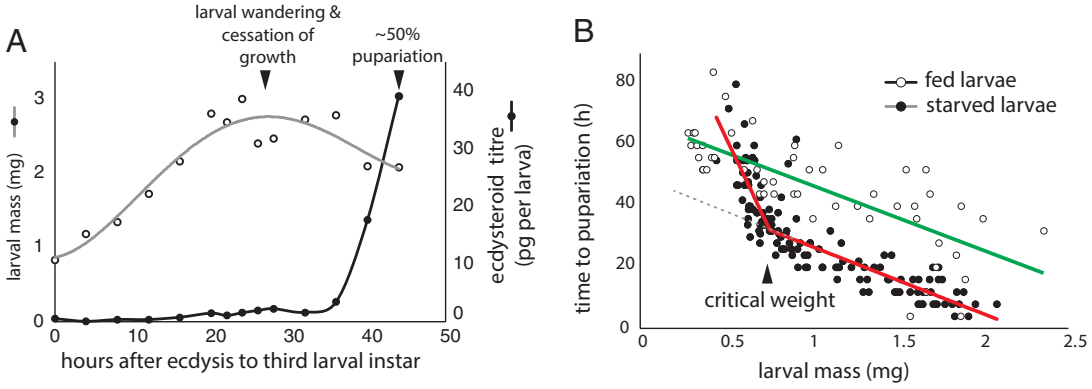

Fig. 1. Growth, physiology, and CW in third-instar Drosophila larvae. (*A*) Growth and ecdysteroid levels during the third larval instar. Data from ref. 39. (*B*) Starvation accelerates pupation in all but the smallest larvae (compare green line to red line). CW (arrow) is marked by a change in the relationship between larval mass at starvation and TTP (gray broken line shows larval mass vs. TTP if there is no change at CW). Data from ref. 36.

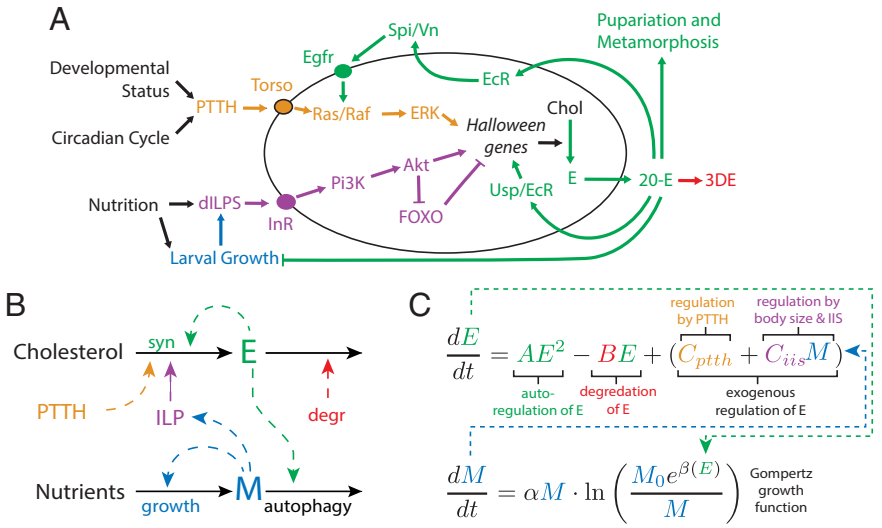

Fig. 2. Mathematical model of growth and ecdysone production during the third instar of *Drosophila* larvae. (*A*) Ecdysone (E) synthesis is up-regulated by the IIS pathway (purple) and the PTTH-signaling pathway (orange). IIS activity is in turn reflective of accumulated body mass (M: blue). After conversion to 20-hydroxyecdysone (20E) in peripheral tissue, ecdysone regulates its own synthesis (green) via PTTH and Usp/EcR signaling. Finally, ecdysteroids are metabolized by ecdysone oxidase to 3DE. See text for details. (*B*) A simplified version of Fig. 2*A* upon which our mathematical model is based. Dotted lines indicate the regulatory relationships captured in our model. (*C*) The differential equations describing ecdysone synthesis and degradation, and the Gompertz function describing growth. The variables are coupled because *M* influences *dE/dt* (blue arrow) and *E* influences *dM/dt* (green arrow). Colors in equations capture regulatory relationships in (*B*). See text for details.

(20E), binds to the ecdysone receptor (EcR) which, with its partner ultraspiracle (Usp), regulates the expression of ecdysone biosynthetic genes (21). Second, 20E activates the secretion of the epidermal growth factor (Egf) ligands spitz and vein by the PG, presumably via EcR (48). These ligands then bind to Egfr in the PG in an autocrine manner and activate the Ras/Raf/MAPK pathway to upregulate ecdysteroidgenesis. Supporting the role of the autoregulation of ecdysone synthesis in the critical-weight phenomenon is the observation that the phenomenon is eliminated in ecdysone-fed larvae; that is, starvation never retards pupation in larvae that are fed ecdysone (21). Finally, 20E is inactivated through at least two mechanisms: conversion by ecdysone oxidase to 3-dehydroecdysone (3DE) (49) and conversion by the cytochrome P450 enzyme Cyp18a1 to 20,26-dihydroxyecdysone (50, 51).

A conceptual model of CW. In summary, 1) the decision to stop growing appears to be a response to nutrient-dependent growth up to a CW; 2) nutrient-dependent growth and ecdysteroidogenesis are positively regulated by IIS; 3) after attainment of CW, pupation is no longer retarded by reduced IIS activity; and 4) ecdysone positively regulates its own synthesis. These observations suggest that, when larvae attain CW, they switch the regulation of ecdysone synthesis from exogenous factors (IIS and PTTH) to the autogenous self-activation pathway (involving 20E and EcR). Here, we present a mathematical model of this hypothesis to determine whether it can account for the critical-weight phenomenon and the decision to metamorphose in *Drosophila* larvae. Our model is based on a very simple, abstract representation (Fig. 2*B*) of the physiological and biochemical data that we have reviewed here.

Ecdysone Dynamics. Based on Fig. 2*B*, which summarizes a host of experimental results (Fig. 2*A*), we assume

1. Ecdysone is synthesized at a rate $C = C_{\text{ptth}} + C_{\text{iis}}$, where C_{ptth} is the contribution to ecdysone synthesis by PTTH and C_{iis} is the contribution by the IIS pathway. For now, we assume that C is a constant (units of pg h^{-1}), but in later subsections, we will account for the influence of larval nutrition and growth on the IIS pathway.
2. Ecdysone is also synthesized by a self-activating pathway (through EcR), at a rate $A{\times}E^2$, where E = ecdysone titer (pg/larva, or "pg" for simplicity) and A is a second-order rate constant (pg^{-1} h^{-1}). Our rate law, $A{\times}E^2$, assumes that the self-activating pathway is a cooperative process and that the larva pupates before $E(t)$ begins to saturate the pathway.
3. Ecdysone is degraded by first-order kinetics, $-B{\times}E$, where B is a first-order rate constant (h^{-1}).

With these assumptions, we write the net rate of change of ecdysone concentration as:

$$\frac{dE}{dt} = AE^2 - BE + C, \qquad [1]$$

where t is time (h). Eq. **1** has a "steady-state" solution whenever $dE/dt = AE^2 - BE + C = 0$ (Fig. 3*A*). For $0 < C < B^2/4A$, $dE/dt = 0$ at two values of E (E_- and E_+), given by the quadratic formula: $E_{\pm} = \frac{B}{2A}\left(1 \pm \sqrt{1 - 4AC/B^2}\right)$. Note that E_- lies between 0 and $B/2A$ and $E_+ > B/2A$. Examining the sign of dE/dt as a function of E (Fig. 3 *A*, *Left*), we see that the lower steady state, E_- (Fig. 3*A*, cyan circle), is stable with respect to small fluctuations of ecdysone concentration; that is, a small increase or decrease in E makes dE/dt negative or positive, respectively, pushing E back to E_-. In contrast, the upper steady-state, E_+ (Fig. 3*A*, magenta circle), is unstable, such that a small increase or decrease in E makes dE/dt positive or negative, respectively, pushing E away from E_+. For $C > B^2/4A$, however, the quadratic equation $dE/dt = 0$ has no real solutions (i.e., no steady states, see Fig. 3 *A*, *Right*). In this case, the ecdysone concentration "blows up" (amplifies rapidly); that is, $E(t) \to \infty$ in finite time, even when ecdysone levels start off very low. These properties of Eq. **1** are illustrated in Fig. 3 *B* and *C*. The value $C = C_{\text{SN}} = B^2/4A$, at which Eq. **1** changes from having two steady-state solutions to having none, is called a "saddle-node bifurcation point" (52). (For more details, see *SI Appendix, Supplementary*

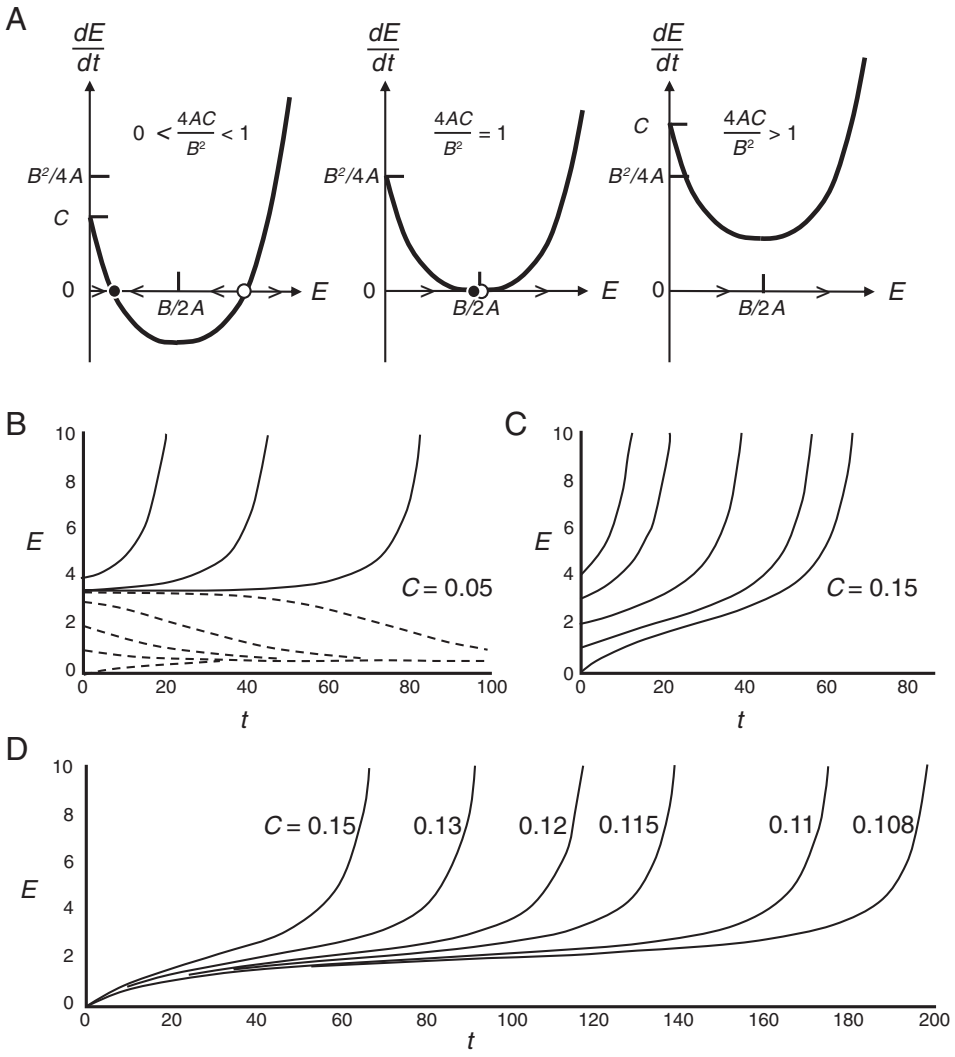

Fig. 3. A saddle-node bifurcation in the dynamics of ecdysone synthesis. (*A*) Steady-state concentrations of ecdysone are given by solutions of $dE/dt = AE^2 - BE + C \equiv F(E) = 0$. *Left*: for $0 \le 4AC/B^2 < 1$, the differential equation for E has both a "stable steady state" (→●←) and an "unstable steady state" (←○→). *Right*: for $4AC/B^2 > 1$, the differential equation for E has no steady state; instead, $E(t) \to \infty$. *Middle*: at $4AC/B^2 = 1$, the stable and unstable steady states merge and annihilate each other. The "saddle-node bifurcation point" at $4AC/B^2 = 1$ separates two regions of qualitatively different behavior. (*B* and *C*) Time courses of $E(t)$ for values of C below and above the saddle-node bifurcation point. Parameter values: $A = 0.025$ and $B = 0.11$, so the saddle-node bifurcation occurs at $C_{SN} = 0.1$. For $C = 0.05$, $E_+ \approx 3.414$, and when the initial value $E \le 3.4$, $E(t)$ decreases to the stable steady state at $E_- \approx 0.586$; however, when initial $E \ge 3.43$, $E(t) \to \infty$. For $C = 0.15$, there is no steady state and $E(t)$ always increases rapidly toward infinity, the "blow up" occurring more rapidly the higher the initial value of E. (*D*) Critical slowing down. As C decreases from 0.15 toward $C_{SN} = 0.1$, the delay until blow up increases toward infinity.

Text S1). From a biological perspective, this means that when ecdysone concentration (E) and IIS and PTTH-signaling (C) are low, the system is homeostatic, maintaining a low level of circulating ecdysone. However, if IIS and PTTH-signaling increase above a certain threshold (C_{SN}), the system abandons the low-level homeostatic state and the circulating ecdysone level increases rapidly, driven by a positive feedback loop whereby ecdysone activates its own synthesis (52).

Growth. Gompertz rate laws are often used to model growth in insect larvae and animals and plants in general (53–59):

$$\text{Gompertz Law } \frac{dM}{dt} = \alpha M \cdot \ln\left(\frac{M_0 e^{\beta}}{M}\right), \qquad [2a]$$

$$\text{or } M(t) = M_0 \exp\left[\beta\left(1 - e^{-\alpha t}\right)\right]. \qquad [2b]$$

Here, M_0 (mg) is the larval mass at the start of L3, and the two parameters (α and β) are related to the initial growth rate of a larva, i.e., $M(t) \approx M_0 e^{\alpha\beta t}$ for $t \approx 0$, and to the maximum mass of a larva, i.e., $M_\infty = \lim_{t\to\infty} M(t) = M_0 e^{\beta}$. However, while the Gompertz growth law captures the growth of a larva up to its maximum size, once the larva stops feeding and begins to wander, its mass declines. This is due to autophagy of stored nutrients to drive development and metamorphosis, as well as clearance of the gut (60, 61). Autophagy and gut clearance are induced by ecdysone (35, 61), so we make β a decreasing function of $E(t)$. A Hill function,

$$\beta(E) = \frac{\beta_0 K^n + \beta_1 E^n}{K^n + E^n}, \quad \beta_0 > \beta_1, \qquad [2c]$$

suitably represents the effect of ecdysone accumulation on growth: as $E(t)$ increases, $\beta(E)$ decreases from β_0 to $\beta_1 < \beta_0$, i.e., the limiting mass, $M_0 e^{\beta}$, of the wandering larva decreases as E increases. The resulting model captures the observed growth dynamics of third instar larvae (Fig. 4*A*).

Ecdysone Dynamics and Growth in Fed Larvae. Combining Eqs. **1** and **2**, we have a mathematical model for larval growth and ecdysone levels:

$$\frac{dE}{dt} = AE^2 - BE + C_{\text{ptth}} + C_{\text{iis}}M, \qquad [\mathbf{3a}]$$

$$\frac{dM}{dt} = \alpha M \cdot \ln\left(\frac{M_0 e^{\beta(E)}}{M}\right), \qquad [\mathbf{3b}]$$

$$\beta(E) = \frac{\beta_0 K^n + \beta_1 E^n}{K^n + E^n}, \quad \beta_0 > \beta_1. \qquad [\mathbf{3c}]$$

To couple ecdysone levels to larval growth, we assume that $C = C_{\text{ptth}} + C_{\text{iis}}M$; that is, C increases with larval mass. We assume that, at the onset of the third larval instar ($t = 0$), $C_{\text{ptth}} + C_{\text{iis}}M_0 < B^2/4A$, so that $E(t)$ is attracted to the stable steady state, $E_- = \frac{B}{2A}\left(1 - \sqrt{1 - 4AC/B^2}\right)$. The growing larva eventually reaches mass M_{SN}, when $C_{\text{ptth}} + C_{\text{iis}}M_{\text{SN}} = B^2/4A$. Hence, $M_{\text{SN}} = \frac{1}{C_{\text{iis}}}\left(\frac{B^2}{4A} - C_{\text{ptth}}\right)$ is the larval mass at the saddle-node bifurcation point. When M exceeds M_{SN}, the stable steady state disappears by coalescing with the unstable steady state (Fig. 3*C*), and $E(t)$ increases, slowly at first and then explosively. Thus, it is growth of the larvae that, via IIS, pushes the level of ecdysone above the saddle-node bifurcation point and causes ecdysone to rapidly increase, albeit after some delay. The irreversible commitment to pupation occurs at M_{SN}, the larval mass at the saddle-node bifurcation point.

In combination, Eqs. **3a**–**3c** can be used to describe changes in body mass and ecdysone titer throughout the third larval instar. Fig. 4*A* illustrates how the model can be fit to experimental data of growth (36, 39) and ecdysone levels (39). The parameter values for this simulation are provided in Table 1. (In order to consolidate data collected from different studies, we have standardized the time scale such that the duration of the third larval instar is 60 h for all the data.) We then used the parameterized model to calculate the TTP for growing larvae at increasingly large sizes, which also closely fits the experimental data (Fig. 4*B*, cyan lines).

Starvation and the Time to Pupation. The critical-weight phenomenon is operationally defined as a change in the effect of starvation on the TTP (Fig. 1*B*). We therefore explored whether our model could capture the effects of starvation on TTP in larvae of different sizes.

To model the effects of starvation, we modify Eq. **3b** with a "feeding function" $F(t)$:

$$\frac{dM}{dt} = \alpha M \cdot \ln\left(\frac{M_0 e^{\beta(E)}}{M}\right) \times F(t), \qquad [\mathbf{3b'}]$$

$$\text{where } F(t) = \text{Heav}\left(T_{\text{starve}} - t\right) = \begin{cases} 1, \text{if } 0 < t < T_{\text{starve}} \\ 0, \text{if } t \geq T_{\text{starve}} \end{cases}$$

An added nuance is that starvation in *Drosophila* larvae that have ostensibly passed CW both increases levels of circulating ecdysone (63) and accelerates pupation (compare TTP for 1 mg larvae that are subsequently starved versus allowed to feed in Fig. 1*A*). These effects are correlated because, as Eq. **1** predicts, once the saddle-node bifurcation has been passed and there is no steady state of E, higher levels of E will cause E to blow up sooner (Fig. 2 *B* and *C*). Therefore, by increasing levels of circulating ecdysone, starvation reduces TTP and promotes early maturation of malnourished larvae. There are three ways to increase ecdysone level: by increasing ecdysone synthesis (*C*), increasing autoregulatory feedback (*A*), or decreasing ecdysone degradation (*B*). For simplicity, we chose to model the effects of starvation by modifying *B* and *C*. To this end, we rewrite Eq. **3a**:

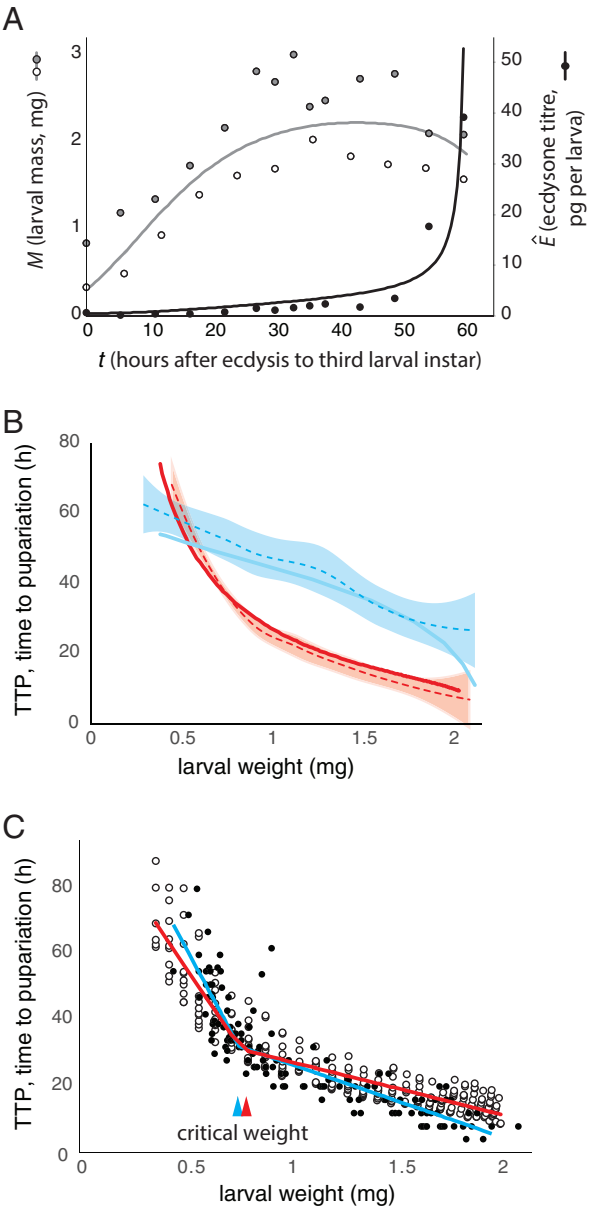

Fig. 4. Model simulations. (*A*) Observed (points) and simulated (lines) relationship between larval mass (gray and white circles) and ecdysone titer (black circles) against larval age. Mass measurements are from ref. 39 (grey circles) and ref. 62 (white circles) and ecdysone titers from ref. 39. Simulations derived from Eqs. **3a**–**3c** using parameter values in Table 1. Time scales have been standardized so that the duration of the instar is 60 h across all datasets. (*B*) Observed (broken line, shading) and simulated (solid line) relationship between larval weight and TTP for fed (cyan) and starved (red) larvae of different weights. The observed trends are Loess regressions fit to the data shown in Fig. 1*B* (36), along with their 95% CIs. The simulated trends are the predicted TTP based on Eqs. **3a**′, **3b**′, and **3c** and Table 1. (*C*) Stochastic TTP simulations for larvae starved at different weights (○) are remarkably congruent with observed data (●). Fitting a segmented linear regression to the observed data (cyan line) and simulated data (red line) predicts CWs (arrows) that are statistically indistinguishable.

Table 1. Model variables, biological correlates, and values

Parameter	Meaning	Value
A	Rate const for ecdysone auto-activation ($pg^{-1}\ h^{-1}$)	0.0225
α	α^{-1} (h) is the time const for Gomperz growth	0.09
B	Rate const for ecdysone degradation in fed larvae (h^{-1})	0.12
B_{st}	Rate const for ecdysone degradation in starved larvae (h^{-1})	0.0875
β	e^{β} is asymptotic mass for Gompertz growth	
β_0	Value of β when E is small (≈0)	2.1
β_1	Value of β when E is large ($\gg K$); $\beta_1 < \beta_0$	1.5
C	Rate const for ecdysone synthesis = $C_{ptth} + C_{iis}M$ ($pg\ h^{-1}$)	
C_{ptth}	PTTH contribution to E synthesis while feeding	0.018
$C_{ptth}{}^{st}$	PTTH contribution to E synthesis when starved	0.036
C_{iis}	IIS contribution to E synthesis while feeding	0.12
$C_{iis}{}^{st}$	IIS contribution to E synthesis when starved	0.24
E_0	Initial concentration of ecdysone per larvae (pg)	0.496
E_{pup}	Ecdysone concentration at pupation	25
K	Ecdysone concentration when $\beta(E) = (\beta_0+\beta_1)/2$	10
M_0	Mass at ecdysis to L3 (mg)	0.3
M_{SN}	Mass at saddle node bifurcation for starved larvae (mg)	0.2
n	Hill exponent for $\beta(E)$ function	2

$$\frac{dE}{dt} = AE^2 - B(t)E + C(t),$$

$$B(t) = B \cdot F(t) + B^{st} \cdot (1 - F(t)), \qquad [\mathbf{3a'}]$$

$$C(t) = \left(C_{ptth} + C_{iis}M\right) \cdot F(t) + \left(C^{st}_{ptth} + C^{st}_{iis}M\right) \cdot (1 - F(t)),$$

where B, C_{ptth}, and C_{iis} are the parameter values for fed larvae, and B^{st}, C^{st}_{ptth}, and C^{st}_{iis} are the values for starved larvae. From simulations of Eqs. **3a′**, **3b′**, and **3c** we can model the relationship between larval mass and time to pupation in larvae that are starved at different masses. We used the same parameter values as for fed larvae but decreased B (ecdysone degradation) and increased C_{ptth} and C_{iis} when larvae are starved (Table 1). Fig. 4*B* shows that model simulations agree very well with experimental TTP vs. mass data (36) for both well-fed and starved larvae.

To understand the relationship between TTP and mass at starvation in our simulation (solid red line in Fig. 4*B*) recall that $C^{st} = C^{st}_{ptth} + C^{st}_{iis}M^{st}$, where C^{st} and M^{st} are the rate of ecdysone synthesis and mass at starvation, respectively. If M^{st} is small enough that $C^{st}_{ptth} + C^{st}_{iis}M^{st} < B^2/4A$, then $E(t)$ will stay at the low stable steady state, $E_- = \frac{B}{2A}\left(1 - \sqrt{1 - 4AC^{st}/B^2}\right)$, and the larva will not pupate. If $M^{st} > M_{SN} \equiv \frac{1}{C^{st}_{iis}}\left(\frac{B^2}{4A} - C^{st}_{ptth}\right)$, the starved larva will, in theory, eventually pupariate. For our parameter values (Table 1), $M_{SN} \approx 0.2$ mg, so even larvae starved at the onset of L3 (with $M_0 = 0.33$ mg) should pupate. However, if M^{st} is just slightly larger than M_{SN}, there will be a long delay to pupate because, close to the saddle-node bifurcation, $E(t)$ increases only very slowly. This effect—called "critical slowing down"—is a generic property of saddle-node bifurcations (see Fig. 3*D* and section 4.3 of ref. 52). In our case, the model predicts TTP > 100 h for $M^{st} = 0.33$ mg. For such a long delay, these larvae would likely die of starvation before they can pupariate. Consequently, there is a MVW below which larvae fail to pupariate, and where MVW > M_{SN}. In Fig. 4*B*, MVW ≈ 0.4 mg (for both observed and simulated data), corresponding to a TTP of ~90 h.

Modeling CW. On the basis of these simulations, we propose that the CW phenomenon reflects a switch in the regulation of ecdysone from exogenous (IIS and PTTH) to endogenous (E and EcR) factors. Our model closely captures the observed growth rate of third-instar larvae (Fig. 2*A*), the changes in the ecdysone titer (Fig. 2*A*), and the relationship between mass and TTP for fed and starved larvae (Fig. 2*B*). Our model also incorporates a switch in the regulation of ecdysteroidgenesis, albeit one that is an emergent property of the system dynamics, which occurs at $M_{SN} \approx 0.2$ mg, the mass at the saddle-node bifurcation point. Puzzlingly, this mass is well below the observed CW of 0.7 to 0.9 mg (36, 64). Further, even though our model incorporates a switch in the regulation of ecdysone synthesis, it does not generate a distinct shift in the relationship between larval mass at starvation and TTP, which is the operational definition of the CW phenomenon (36, 65). Rather, the relationship between larval mass at starvation and TTP in our model declines continuously as (approximately) a negative power function (Fig. 4*B*). How then can we reconcile the observations that our model closely captures experimental data but does not include a mechanistic correlate of CW?

CW in *Drosophila* is statistically determined by fitting a two-interval segmented regression in order to capture the apparent change in the linear relationship between mass at starvation and TTP before and after CW (Fig. 1*B*) (21, 36, 62, 64–66). The break-point in the segmented regression is the CW. We can therefore explore whether applying a segmented regression to data simulated by our model predicts a CW close to that observed for experimental data.

Biological data are inherently noisy and our model is not. To simulate biological noise, we assume that the value of C_{iis} varies from one larva to the next in a random manner, as follows:

$$C^{(i)}_{iis} = C^{(0)}_{iis} \cdot r_i, \ \ i = 1, \ 2, \ \ \ldots, \qquad [\mathbf{4}]$$

where C_{iis}^{0} is the value of C_{iis} in the deterministic simulation, and the r_i's are random numbers drawn from a uniform distribution over $[1 - \Delta C_{iis}, 1 + \Delta C_{iis}]$. To fit the observed distributions of data points, we choose $\Delta C_{iis} = 0.25$. Note that, for simplicity, we are subsuming the effects of measurement error into the intrinsic variability of C_{iis}. In this simulation we assume that larvae that take longer than 90 h to pupate die before they can do so. To match experimental data (36), we also only simulated TTP in larvae <2 mg, which is peak larval mass. As shown in Fig. 4*C*, stochastic TTP simulations for starved larvae are remarkably congruent with experimental data. More importantly, fitting a two-interval segmented regression to the simulated data (67) indicates a CW = 0.77 mg, statistically indistinguishable from the observed CW = 0.76 mg (95% CI: 0.72 to 0.80) (36). Thus, the model can generate a critical-weight phenomenon without a direct mechanistic correlate for it. In our model, CW is a statistical epiphenomenon associated with the "speeding up" of the dynamical system as it moves away from the saddle-node bifurcation point. In contrast, the MVW is a reflection of the saddle-node bifurcation and therefore does have a mechanistic correlate.

Effects of Mutations on Growth and Ecdysone Levels. Several groups have studied the effects of down- or up-regulating proteins involved in ecdysone metabolism and their effects on CW or the timing of pupation. For example, increasing the expression of the genes that positively regulate ecdysteroidogenesis via IIS or PTTH signaling—such as *Ras*, *Raf*, and *Pi3K*—causes precocious pupation, through a reduction in MVW (44, 46, 47). In contrast, decreasing the expression of these genes has the opposite effect.

In our model, the effects of IIS and PTTH signaling on ecdysteroidogenesis are mediated by the parameters C_{iis} and C_{ptth}, respectively. We therefore investigated the effects of changing the value of either of these parameters on the duration of L3 (Fig. 5). As expected, increasing either C_{iis} or C_{ptth}, and thus simulating an increase in ecdysone synthesis, decreases MVW and CW and advances pupation, whereas decreasing these parameters has the opposite effect, consistent with experimental data. The timing of pupation is more sensitive to changes in C_{iis} than changes in C_{ptth}. Intriguingly, setting $C_{iis} = 0$, which simulates the complete inhibition of IIS, prevents pupation, while setting $C_{ptth} = 0$, which simulates the complete inhibition of PTTH signaling, delays pupation but does not prevent it. This is consistent with experimental data on the suppression of IIS and PTTH signaling in the PG: Strong suppression of IIS in the PG causes larval death (46), whereas complete elimination of PTTH signaling merely causes developmental delay (44).

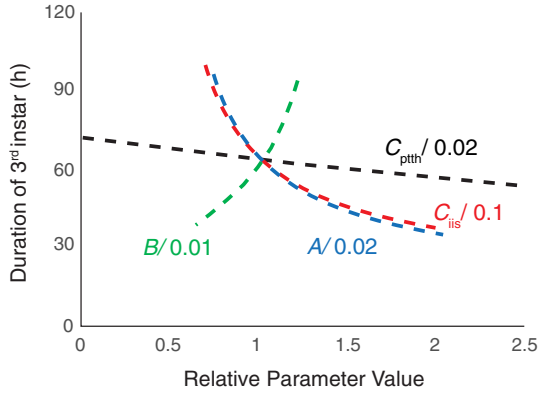

Fig. 5. The effect of up- or down-regulating ecdysone production and clearance on developmental time. *A* = level of ecdysone auto-regulation, *B* = rate of ecdysone clearance, C_{ptth} = activity of PTTH pathway, C_{iis} = activity of IIS pathway. In this simulation, the nominal values of these parameters for "wild type" larvae are $A = 0.02$, $B = 0.1$, $C_{ptth} = 0.02$, $C_{iis} = 0.1$. See Table 1 for other parameter values.

Our model predicts that a reduction in the rate (*A*) of autogenous production should increase MVW and CW and delay pupation whereas an increase in *A* will have the opposite effect (Fig. 5). A key component of the autogenous production of ecdysone is the ecdysone receptor, EcR, and experimental data show that, consistent with our model, knockdown of *EcR* and its binding partner *Usp* causes substantial developmental delay (68). Mutations that interfere with other aspects of the autogenous production of ecdysone have similar effects (48, 69). Unexpectedly, the quantitative effect of changing A/A_{WT} is nearly identical to the effects of changing the strength of IIS signaling, $C_{iis}/C_{iis,WT}$.

Finally, our model also predicts that increasing ecdysone clearance, *B*, should delay pupation. There are, however, little data to support this prediction. The degradation of ecdysone has not been so intensely studied as its synthesis. However, loss of *CYP18A1*, a key enzyme of *Drosophila* steroid-hormone inactivation, actually delays pupation rather than accelerates it (50), an observation that is difficult to reconcile with our model and that warrants further investigation.

Discussion

The decision to stop growth regulates adult body size and is fundamental to animal form and function. In many animals, the decision to stop growing is coincident with the release of steroid hormones that systemically coordinate developmental maturation. The precise mechanisms that trigger the release of these hormones remain poorly understood, although they are thought to reflect attainment of a particular body size or condition, implicating a size-sensing mechanism in the decision to stop growth. In this paper, we describe a mathematical model of the mechanisms that regulate the timely release of the steroid hormone ecdysone in *D. melanogaster*, which ultimately causes the cessation of larval growth, initiates metamorphosis, and determines adult body size at pupation. Our model precisely captures the relationship between starvation and the timing of pupation in *Drosophila* and predicts a CW statistically indistinguishable from that observed in experimental data. Our model supports our hypothesis that the decision to stop growing in *Drosophila* is regulated by a switch from exogenous to endogenous regulation of ecdysone synthesis by the PG. This switch is marked by a saddle-node bifurcation in the dynamics of the equations that describe ecdysteroidgenesis, with growth and a correlated increase in nutritional signaling pushing the system across the bifurcation point. Intriguingly, however, this switch in ecdysone regulation at M_{SN} (mass at the saddle-node bifurcation) occurs well before attainment of CW; that is, $M_{SN} <$ CW. Indeed, the switch is reflective of the MVW for pupation. Thus, the critical-weight phenomenon is an indirect consequence of the mechanism by which body size—specifically larval mass at the saddle-node bifurcation point—induces an irreversible commitment to metamorphosis. Indeed, the observation of CW is a consequence of "critical slowing down" of ecdysone synthesis for larval masses marginally larger than M_{SN}.

If our model proves correct, it provides an elegant solution to how *Drosophila* decides to end growth and pupate at the correct size: a larva initiates steroid synthesis when IIS signaling in the PG rises above a threshold and ecdysone synthesis becomes self-regulating. As long as IIS in the PG is correlated with a larva's size and nutritional status, this will reliably ensure that a larva does not pupate at an inappropriate size. We have explicitly incorporated a

positive correlation between larval mass and IIS in our model, such that the IIS increases with larval growth (Eq. **3a**). Alternatively, IIS may be constant but drive correlated growth of the PG and the body, with ecdysone synthesis increasing linearly with PG size. Experimental evidence favors the former hypothesis. FOXO, a negative regulator of IIS, directly interacts with Ultraspiracle (Usp), part of the ecdysone receptor, and together they suppress ecdysteroidogenesis (21). Overexpressing FOXO delays attainment of CW and the expression of ecdysone biosynthesis genes, which is partially rescued by disrupting the association between FOXO and Usp (21). Importantly, FOXO activity is suppressed by IIS (42, 70). This suggests that, as IIS increases during the third larval instar, FOXO is progressively inactivated and dissociates from the FOXO–Usp complex to cause an increase in ecdysone synthesis.

Our model challenges a mechanistic basis for CW in *Drosophila*, a phenomenon that has been studied for at least 80 y (71). This does not mean that CW does not exist in fruit flies. Rather, we argue that the phenomenon is reflective of a decision to pupariate made earlier in development. This means that we should not necessarily focus on the physiological events occurring around attainment of CW to elucidate the mechanism *Drosophila* larvae use to initiate the cessation of growth. For example, several studies have identified small peaks in ecdysone (21) and 20E (39) 8 to 10 h after ecdysis to the third instar and coincident with attainment of CW. Our model suggests that these peaks in E and 20E may be a consequence of changes in the regulation of ecdysone synthesis made earlier in the larval instar.

Our model also does not mean that CW is not evolutionarily or ecologically important. For a fruit fly larva living in an ephemeral nutritional environment, the size at which no further nutrition is necessary to make it to adulthood without substantial delay is an important milestone. This is a life-history characteristic that will be subject to selection, even if the mechanisms that regulate CW are responding to a developmental decision earlier in development. Thus, natural selection can affect CW by targeting genes that underlie the parameters in our model.

The physiology of the CW phenomenon has been best elucidated in *M. sexta*, where the term *CW* was first coined (37). Here, starvation before CW retards development but starvation after CW does not accelerate development, such that fed and starved larvae initiate metamorphosis at the same time. Attainment of CW is followed by a rapid decline in circulating juvenile hormone, which derepresses PTTH secretion from the brain, resulting in an increase in ecdysone synthesis (72, 73). PTTH secretion is also photoperiodically regulated, so that it can only occur during a photoperiod gate which, for a 12D:12L photoperiod, extends from lights off until early in the next light phase (74). Further, larvae must achieve CW at least 24 h before the opening of this photoperiodic gate in order to release PTTH (5). This is quite different from the CW phenomenon in *Drosophila*, which is not dependent on juvenile hormone (75) and does not appear to be photoperiodically gated. Thus, an open question is whether the CW phenomenon in *M. sexta* has a mechanistic basis that relies on an as yet unresolved size-assessment signal, or whether, like *Drosophila*, such a mechanism is not necessary to generate the CW phenomenon.

One possibility is that the ostensibly simple CW mechanism in *Drosophila* represents a core system that has been evolutionarily stripped of peripheral regulators to prioritize rapid development. Other insects may have additional levels of control, including mechanisms that more directly sense body size, such that this core system is only used redundantly under conditions that restrict growth. For example, in *M. sexta*, larvae that are starved or hypoxic never achieve CW but are nevertheless able to pupate as long as they are above the MVW (22, 76). The leaky PG hypothesis (22, 77) proposes that pupation in these larvae is achieved by the slow and prolonged release of ecdysone from a "leaky" PG, independent of PTTH. In our model, *Drosophila* larvae starved below their CW but above MVW are able to eventually pupate because the "switch" that initiates ecdysone synthesis has already occurred. If the same core-system exists in *M. sexta*, the leaky PG may be a PG that has already irreversibly committed to ecdysone synthesis, albeit with considerable delay. Under normal growth conditions, however, additional size-sensing signals that work via PTTH may override this core system, causing ecdysone levels to peak and induce metamorphosis on a normal schedule. The support for this explanation of the leaky PG comes from the observation that attainment of MVW in both *M. sexta* and *Drosophila* is marked by the initiation of nutrient-independent growth of the PG cells and by increased expression of ecdysone biosynthesis genes, presumably independently of PTTH (76).

Our model is clearly a simplification of the physiological mechanisms used to initiate pupation in *Drosophila*. In particular, it does not generate the characteristic pulses of ecdysteroids that drive the developmental changes leading up to pupation—including puffing of the salivary gland chromosomes and larval wandering—that are reproduced in myriad insect physiology texts. Importantly, however, these pulses are in the concentration of 20E, which is derived from ecdysone by the enzyme Shade in peripheral tissue. The total ecdysteroid titer (including metabolic derivatives of E) increases steadily throughout the third larval instar, before dramatically increasing at pupation (Fig. 1*A*) (39). This steady increase is, however, punctuated by smaller fluctuations that coincide with the more discrete pulses of 20E (39) and which appear to reflect the periodicity of PTTH synthesis that is not included in our model (44). These small fluctuations do not seem to be temporary deviations from the low-level homeostatic state predicted by our model (Fig. 3*B*) because the pulses occur after the PG has irreversibly committed to the rapid increase in ecdysteroidogenesis that causes pupation. Thus, while the increase in ecdysone synthesis may be caused by pulses of PTTH, some additional mechanism must arrest ecdysone synthesis to generate a subsequent decline. It is interesting to note that the timely release of ecdysone is also dependent on a circadian clock in the PG itself. This clock is regulated not only by PTTH-producing neurons, which are anatomically closely associate with clock neurons in the brain (44, 78), but also by IIS (79). Future iterations of the model could include additional levels of temporal control to explore whether they are sufficient to generate fluctuations in ecdysone synthesis. Additional experiments that explore whether the pulses of ecdysone and 20E are maintained in larvae that lack PTTH (44) are also essential.

Nonetheless, while PTTH is clearly important for the timely release of ecdysone and pupation, experimental data as well as our model indicate that while larvae without PTTH-signaling can still metamorphose, albeit with delay, this is not true for IIS. Thus, the IIS pathway appears primary in the mechanism that controls the timing of ecdysteroidogenesis, the duration of growth, and adult body size.

In conclusion, our model provides a simple mechanism to coordinate the timely release of a steroid hormone with attainment of a particular body size that does not rely on a body size-sensing mechanism to directly trigger hormone synthesis. Rather, hormone release is a consequence of the correlation of growth and nutritional signaling pushing steroid synthesis above a threshold whereby it autoregulates its own synthesis. Consequently, animals do not necessarily need to be able to assess their own body size to reliably initiate maturation at a particular size even if they appear to do so. Steroid hormones drive maturation and stop growth in a wide diversity of animals, including humans, in which the onset of puberty has also been proposed to be associated with the attainment

of CW (9, 80). Further, the IIS pathway is highly conserved and regulates nutrition-dependent growth in almost all animals. Our model therefore provides a framework for understanding how nutritional and steroid signaling regulate maturation and the cessation of growth in animals in general, albeit a framework upon which additional regulators of developmental timing may be built.

Materials and Methods

All the simulations in this paper were generated using either XPP-Auto (81) or Simulink/Matlab. Parameter values were estimated by simulating the ecdysone titre through time, growth curves and the relationship between age and TTP for fed and starved larvae, and comparing these simulations with the observed experimental data from refs. 36 and 39. Loess regression and segmented linear regression were fitted to the simulated data using the *stats* and *segmented* packages in *R*, respectfully (67, 82). The XPP-Auto and Simulink/Matlab scripts used to run the simulations, the observed experimental and simulated data, and the *R* scripts used to analyze these data, are provided in the *SI Appendix* and on Dryad (83).

Data, Materials, and Software Availability. Code data have been deposited in Dryad (83).

ACKNOWLEDGMENTS. We would like to thank members of the Shingelton Laboratory, Christen Mirth and Viviane Callier for their comments on early drafts of the MS. A.W.S. was supported by NSF IOS–1952385. S.Y.S. was supported by R01 HD085870/HD/NICHD NIH HHS/United States.

1. M. LaBarbera, Analyzing body size as a factor in ecology and evolution. *Annu. Rev. Ecol. Syst.* **20**, 97–117 (1989).
2. A. M. Nevill, R. Ramsbottom, C. Williams, Scaling physiological measurements for individuals of different body size. *Eur. J. Appl. Physiol. Occup. Physiol.* **65**, 110–117 (1992).
3. T. M. Plant, Neuroendocrine control of the onset of puberty. *Front. Neuroendocrinol.* **38**, 73–88 (2015).
4. C. G. Barredo, B. Gil-Marti, D. Deveci, N. M. Romero, F. A. Martin, Timing the juvenile-adult neurohormonal transition: Functions and evolution. *Front. Endocrinol.* **11**, 602285 (2021).
5. H. F. Nijhout, Physiological control of molting in insects. *Integr. Comp. Biol.* **21**, 631–640 (1981).
6. B. K. Follett, "The Physiology of Puberty in Seasonally Breeding Birds" in *Follicle Stimulating Hormone*, M. Hunzicker-Dunn, N. B. Schwartz, Eds. (Springer, 1992), pp. 54–65.
7. B. Paul, Z. R. Sterner, D. R. Buchholz, Y.-B. Shi, L. M. Sachs, Thyroid and corticosteroid signaling in amphibian metamorphosis. *Cells* **11**, 1595 (2022).
8. S. Livadas, G. P. Chrousos, Molecular and environmental mechanisms regulating puberty initiation: An integrated approach. *Front. Endocrinol.* **10**, 828 (2019).
9. M. Bygdell, J. M. Kindblom, J.-O. Jansson, C. Ohlsson, Revisiting the critical weight hypothesis for regulation of pubertal timing in boys. *Am. J. Clin. Nutr.* **113**, 123–128 (2021).
10. L. Huang *et al.*, Critical body fat percentage required for puberty onset: The Taiwan Pubertal Longitudinal Study. *J. Endocrinol. Investig.* **46**, 1177–1185 (2023).
11. M. C. Manotas, D. M. González, C. Céspedes, C. Forero, A. P. R. Moreno, Genetic and epigenetic control of puberty. *Sex. Dev.* **16**, 1–10 (2022).
12. R. Renema, F. Robinson, M. Newcombe, R. McKay, Effects of body weight and feed allocation during sexual maturation in broiler breeder hens. 1. Growth and carcass characteristics. *Poult. Sci.* **78**, 619–628 (1999).
13. Y. E. Morbey, D. Pauly, Juvenile-to-adult transition invariances in fishes: Perspectives on proximate and ultimate causation. *J. Fish Biol.* **101**, 874–884 (2022).
14. H. I'Anson, D. L. Foster, G. R. Foxcroft, P. J. Booth, Nutrition and reproduction. *Oxf. Rev. Reprod. Biol.* **13**, 239–311 (1991).
15. G. C. Kennedy, J. Mitra, Body weight and food intake as initiating factors for puberty in the rat. *J. Physiol.* **166**, 408–418 (1963).
16. H. F. Nijhout *et al.*, The developmental control of size in insects. *Wiley Interdiscip. Rev. Dev. Biol.* **3**, 113–134 (2014).
17. Y. Suzuki, T. Koyama, K. Hiruma, L. M. Riddiford, J. W. Truman, A molt timer is involved in the metamorphic molt in Manduca sexta larvae. *Proc. Natl. Acad. Sci. U.S.A.* **110**, 12518–12525 (2013).
18. M. J. Texada, T. Koyama, K. Rewitz, Regulation of body size and growth control. *Genetics* **216**, 269–313 (2020).
19. B. R. Helm, J. P. Rinehart, G. D. Yocum, K. J. Greenlee, J. H. Bowsher, Metamorphosis is induced by food absence rather than a critical weight in the solitary bee, Osmia lignaria. *Proc. Natl. Acad. Sci. U.S.A.* **114**, 10924–10929 (2017).
20. P. T. Rohner, W. U. Blanckenhorn, M. A. Schäfer, Critical weight mediates sex-specific body size plasticity and sexual dimorphism in the yellow dung fly Scathophaga stercoraria (Diptera: Scathophagidae). *Evol. Dev.* **19**, 147–156 (2017).
21. T. Koyama, M. A. Rodrigues, A. Athanasiadis, A. W. Shingleton, C. K. Mirth, Nutritional control of body size through FoxO-Ultraspiracle mediated ecdysone biosynthesis. *Elife* **3**, e03091 (2014).
22. V. Callier, H. F. Nijhout, Control of body size by oxygen supply reveals size-dependent and size-independent mechanisms of molting and metamorphosis. *Proc. Natl. Acad. Sci. U.S.A.* **108**, 14664–14669 (2011).
23. J. R. Kannangara, C. K. Mirth, C. G. Warr, Regulation of ecdysone production in Drosophila by neuropeptides and peptide hormones. *Open Biol.* **11**, 200373 (2021).
24. S. Huang, Y.-P. Guo, G. May, T. Enver, Bifurcation dynamics in lineage-commitment in bipotent progenitor cells. *Dev. Biol.* **305**, 695–713 (2007).
25. L. D. Mot *et al.*, Cell fate specification based on tristability in the inner cell mass of mouse blastocysts. *Biophys. J.* **110**, 710–722 (2016).
26. J. J. Tyson, R. Albert, A. Goldbeter, P. Ruoff, J. Sible, Biological switches and clocks. *J. R. Soc. Interface* **5**, S1–S8 (2008).
27. T. Hong, J. Xing, L. Li, J. J. Tyson, A simple theoretical framework for understanding heterogeneous differentiation of CD4+ T cells. *BMC Syst. Biol.* **6**, 66 (2012).
28. X.-J. Tian, H. Zhang, J. Xing, Coupled reversible and irreversible bistable switches underlying TGFβ-induced epithelial to mesenchymal transition. *Biophys. J.* **105**, 1079–1089 (2013).
29. J. J. Tyson *et al.*, Time-keeping and decision-making in living cells: Part II. *Interface Focus* **12**, 20220024 (2022).
30. J. J. Tyson, K. C. Chen, B. Novak, Sniffers, buzzers, toggles and blinkers: Dynamics of regulatory and signaling pathways in the cell. *Curr. Opin. Cell Biol.* **15**, 221–231 (2003).
31. J. E. Ferrell, *Systems Biology of Cell Signaling, Recurring Themes and Quantitative Models* (Garland Science, 2021), pp. 147–161.
32. J. E. Ferrell, *Systems Biology of Cell Signaling, Recurring Themes and Quantitative Models* (Garland Science, 2021), pp. 129–145.
33. J. Parker, G. Struhl, Control of Drosophila wing size by morphogen range and hormonal gating. *Proc. Natl. Acad. Sci. U.S.A.* **117**, 31935–31944 (2020).
34. A. N. Alves, M. M. Oliveira, T. Koyama, A. Shingleton, C. K. Mirth, Ecdysone coordinates plastic growth with robust pattern in the developing wing. *Elife* **11**, e72666 (2022).
35. T. E. Rusten *et al.*, Programmed autophagy in the Drosophila fat body is induced by ecdysone through regulation of the PI3K pathway. *Dev. Cell* **7**, 179–192 (2004).
36. B. C. Stieper, M. Kupershtok, M. V. Driscoll, A. W. Shingleton, Imaginal discs regulate developmental timing in Drosophila melanogaster. *Dev. Biol.* **321**, 18–26 (2008).
37. H. F. Nijhout, C. M. Williams, Control of moulting and metamorphosis in the tobacco hornworm, Manduca sexta (L.): Growth of the last-instar larva and the decision to pupate. *J. Exp. Biol.* **61**, 481–491 (1974).
38. G. H. D. Moed, C. L. J. J. Kruitwagen, G. D. Jong, W. Scharloo, Critical weight for the induction of pupariation in Drosophila melanogaster: Genetic and environmental variation. *J. Evol. Biol.* **12**, 852–858 (1999).
39. J. T. Warren *et al.*, Discrete pulses of molting hormone, 20-hydroxyecdysone, during late larval development of Drosophila melanogaster: Correlations with changes in gene activity. *Dev. Dyn.* **235**, 315–326 (2006).
40. W. Brogiolo *et al.*, An evolutionarily conserved function of the Drosophila insulin receptor and insulin-like peptides in growth control. *Curr. Biol.* **11**, 213–221 (2001).
41. O. Puig, M. T. Marr, M. L. Ruhf, R. Tjian, Control of cell number by Drosophila FOXO: Downstream and feedback regulation of the insulin receptor pathway. *Genes Dev.* **17**, 2006–2020 (2003).
42. D. S. Hwangbo *et al.*, Drosophila dFOXO controls lifespan and regulates insulin signalling in brain and fat body. *Nature* **429**, 562–566 (2004).
43. Y. Ohhara, S. Kobayashi, N. Yamanaka, Nutrient-dependent endocycling in steroidogenic tissue dictates timing of metamorphosis in Drosophila melanogaster. *PLoS Genet.* **13**, e1006583 (2017).
44. Z. Mcbrayer *et al.*, Prothoracicotropic hormone regulates developmental timing and body size in Drosophila. *Dev. Cell* **13**, 857–871 (2007).
45. K. F. Rewitz, N. Yamanaka, L. I. Gilbert, M. B. O'connor, The insect neuropeptide PTTH activates receptor tyrosine kinase torso to initiate metamorphosis. *Science* **326**, 1403–1405 (2009).
46. C. Mirth, J. Truman, L. Riddiford, The role of the prothoracic gland in determining critical weight for metamorphosis in Drosophila melanogaster. *Curr. Biol.* **15**, 1796–1807 (2005).
47. P. E. Caldwell, M. Walkiewicz, M. Stern, Ras activity in the Drosophila prothoracic gland regulates body size and developmental rate via ecdysone release. *Curr. Biol.* **15**, 1785–1795 (2005).
48. J. Cruz, D. Martín, X. Franch-Marro, Egfr signaling is a major regulator of ecdysone biosynthesis in the Drosophila prothoracic gland. *Curr. Biol.* **30**, 1547–1554.e4 (2020).
49. H. Takeuchi, D. J. Rigden, B. Ebrahimi, P. C. Turner, H. H. Rees, Regulation of ecdysteroid signalling during Drosophila development: Identification, characterization and modelling of ecdysone oxidase, an enzyme involved in control of ligand concentration. *Biochem. J.* **389**, 637–645 (2005).
50. E. Guittard *et al.*, CYP18A1, a key enzyme of Drosophila steroid hormone inactivation, is essential for metamorphosis. *Dev. Biol.* **349**, 35–45 (2011).
51. K. F. Rewitz, N. Yamanaka, M. B. O'Connor, Steroid hormone inactivation is required during the juvenile-adult transition in Drosophila. *Dev. Cell* **19**, 895–902 (2010).
52. S. H. Strogatz, *Nonlinear Dynamics and Chaos, with Applications to Physics, Biology, Chemistry, and Engineering* (CRC Press, 2019), 10.1201/9780429492563.
53. L. L. He *et al.*, Mechanism of threshold size assessment: Metamorphosis is triggered by the TGF-beta/Activin ligand Myoglianin. *Insect. Biochem. Mol. Biol.* **126**, 103452 (2020).
54. H. F. Nijhout, R. Z. German, Developmental causes of allometry: New models and implications for phenotypic plasticity and evolution. *Integr. Comp. Biol.* **52**, 43–52 (2012).
55. H. F. Nijhout, K. Z. McKenna, Allometry, scaling, and ontogeny of form–An introduction to the symposium. *Integr. Comp. Biol.* **59**, 1275–1280 (2019).
56. R. E. Ricklefs, Embryo growth rates in birds and mammals. *Funct. Ecol.* **24**, 588–596 (2010).
57. J. Vollmer *et al.*, A quantitative analysis of growth control in the Drosophila eye disc. *Development* **143**, 1482–1490 (2016).
58. A. R. Lammers, H. A. Dziech, R. Z. German, Ontogeny of sexual dimorphism in Chinchilla lanigera (Rodentia: Chinchillidae). *J. Mammal.* **95**, 179–189 (2001).
59. K. M. C. Tjørve, E. Tjørve, The use of Gompertz models in growth analyses, and new Gompertz-model approach: An addition to the Unified-Richards family. *PLoS One* **12**, e0178691 (2017).
60. D. Denton, K. Mills, S. Kumar, Chapter 2 methods and protocols for studying cell death in Drosophila. *Methods Enzym.* **446**, 17–37 (2008).
61. K. Tracy, E. H. Baehrecke, The role of autophagy in Drosophila metamorphosis. *Curr. Top. Dev. Biol.* **103**, 101–125 (2013).
62. N. D. Testa, S. M. Ghosh, A. W. Shingleton, Sex-specific weight loss mediates sexual size dimorphism in Drosophila melanogaster. *PLoS One* **8**, e58936 (2013).
63. G. J. Lee *et al.*, Steroid signaling mediates nutritional regulation of juvenile body growth via IGF-binding protein in Drosophila. *Proc. Natl. Acad. Sci. U.S.A.* **115**, 5992–5997 (2018).
64. S. M. Ghosh, N. D. Testa, A. W. Shingleton, Temperature-size rule is mediated by thermal plasticity of critical size in Drosophila melanogaster. *Proc. R. Soc. B Biol. Sci.* **280**, 20130174 (2013).

65. K. Hironaka, K. Fujimoto, T. Nishimura, Optimal scaling of critical size for metamorphosis in the genus Drosophila. *iScience* **20**, 348–358 (2019).
66. V. Callier *et al.*, The role of reduced oxygen in the developmental physiology of growth and metamorphosis initiation in Drosophila melanogaster. *J. Exp. Biol.* **216**, 4334–4340 (2013).
67. V. M. W. Muggeo, segmented: An R package to fit regression models with broken-line relationships. *R News* **8**, 20–25 (2008).
68. A. Mansilla, F. A. Martín, D. Martín, A. Ferrús, Ligand-independent requirements of steroid receptors EcR and USP for cell survival. *Cell Death Differ.* **23**, 405–416 (2016).
69. C. F. Christensen *et al.*, Ecdysone-dependent feedback regulation of prothoracicotropic hormone controls the timing of developmental maturation. *Development* **147**, dev188110 (2020).
70. M. A. Jünger *et al.*, The Drosophila forkhead transcription factor FOXO mediates the reduction in cell number associated with reduced insulin signaling. *J. Biol.* **2**, 20 (2003).
71. G. W. Beadle, E. L. Tatum, C. W. Clancy, Food level in relation to rate of development and eye pigmentation in Drosophila melanogaster. *Biol. Bull.* **75**, 447–462 (1938).
72. D. B. Rountree, W. E. Bollenbacher, The release of the prothoracicotropic hormone in the tobacco hornworm, Manduca sexta, is controlled intrinsically by juvenile hormone. *J. Exp. Biol.* **120**, 41–58 (1986).
73. H. F. Nijhout, C. M. Williams, Control of moulting and metamorphosis in the tobacco hornworm, Manduca sexta (L.): Cessation of juvenile hormone secretion as a trigger for pupation. *J. Exp. Biol.* **61**, 493–501 (1974).
74. J. W. Truman, L. M. Riddiford, Physiology of insect rhythms. 3. The temporal organization of the endocrine events underlying pupation of the tobacco hornworm. *J. Exp. Biol.* **60**, 371–382 (1974).
75. C. K. Mirth *et al.*, Juvenile hormone regulates body size and perturbs insulin signaling in Drosophila. *Proc. Natl. Acad. Sci. U.S.A.* **111**, 7018–7023 (2014).
76. L. C. Xu *et al.*, Distinct nutritional and endocrine regulation of prothoracic gland activities underlies divergent life history strategies in Manduca sexta and Drosophila melanogaster. *Insect Biochem. Mol. Biol.* **119**, 103335 (2020).
77. H. F. Nijhout, The rôle of ecdysone in pupation of Manduca sexta. *J. Insect Physiol.* **22**, 453–463 (1976).
78. M. Selcho *et al.*, Central and peripheral clocks are coupled by a neuropeptide pathway in Drosophila. *Nat. Commun.* **8**, 15563 (2017).
79. F. D. Cara, K. King-Jones, The circadian clock is a key driver of steroid hormone production in Drosophila. *Curr. Biol.* **26**, 2469–2477 (2016).
80. R. E. Frisch, R. Revelle, Height and weight at menarche and a hypothesis of critical body weights and adolescent events. *Science* **169**, 397–399 (1970).
81. B. Ermentrout, A. Mahajan, Simulating, analyzing, and animating dynamical systems: A guide to XPPAUT for researchers and students. *Appl. Mech. Rev.* **56**, B53–B53 (2003).
82. R Core Team, *R: A Language and Environment for Statistical Computing* (R Foundation for Statistical Computing, 2013).
83. A. Shingleton, T. John, A. Monshizadeh, S. Shvartsman, A Dynamical Model of Growth and Maturation in Drosophila [Dataset]. Dryad. https://doi.org/10.5061/dryad.q573n5tq2. Deposited 9 November 2023.